Institute of Space and Aeronautical Science, University of Tokyo
Report No. 404, July 1966

A Gasdynamic Analysis of the Counter-Flow Diffusion Flame in the Forward Stagnation Region of a Porous Cylinder

By

Hiroshi TSUJI and Ichiro YAMAOKA

Summary: In the present paper, a gasdynamic analysis is made on the counter-flow diffusion flame established in the forward stagnation region of a porous cylinder, from the surface of which the fuel gas is ejected uniformly into the uniform air stream, and the effects of the aerodynamic and chemical parameters upon the location of the flame are examined. The flow, concentration and temperature fields are analyzed on the flame sheet model and by the boundary layer approximation. The general analytic expression for the relation between the location of the flame and the fuel ejection rate is obtained, and the location of the flame is determined for various combinations of reactants by a simple calculation. Some of these theoretical results are compared with the experimental results observed by the present authors. It is found that the theoretical results are qualitatively consistent with the observed results, and therefore, the flame sheet model is useful to evaluate the effects of the aerodynamic and chemical parameters upon the location of the flame, although the blow-off limit of the flame observed in the experiment can not be predicted by the flame sheet model in which the infinite rate of reaction is assumed in the flame zone.

1. INTRODUCTION

In an investigation into the burning rates of liquid fuels, it was first observed by Spalding that the diffusion flame which entirely surrounded a liquid fuel sphere suspended in an air stream was suddenly converted into the so-called wake flame as the air stream velocity reached a critical value [*1*] [*2*]. This extinction phenomenon of the counter-flow diffusion flame appears to result from chemical limitations on the combustion rate, and the theories to explain the extinction of such a flame were presented by Spalding [*2*] [*3*], and recently by Fendell [*4*].

In recent years, Potter and his co-workers developed a novel experimental method in which the reactant flow velocity at blow-off of a diffusion flame established in the zone of impingement of two directly opposed gaseous jets of fuel and oxidant was used as a measure of the reaction rate, and the apparent flame strength was measured for various oxidant-fuel combinations [*5*] [*6*] [*7*]. Owing to velocity variations across the burner mouths and other incidental effects, such flames are not flat and blow-off is deemed to occur when the central portion disappears and only a ring of flame remains. The theory of such a flame, or rather an idealization

of it, was considered by Spalding, and the flow conditions under which blow-off could be taken as a criterion of reaction rate were deduced [*8*].

Pandya and Weinberg studied the detailed aerodynamic and thermal structure of a large flat diffusion flame in the counter-flow regime of opposed jets of two gaseous reactants and showed that the establishment of such a flame could considerably extend the range of applicability of flame-kinetics studies by structure analysis [*9*] [*10*]. However, the aerodynamic structure of this flame is rather complicated, and two stagnation points and two planes which particles cannot cross occur when the centers of the reaction and aerodynamic systems are made to coincide.

An experimental study has been conducted by the present authors on the laminar, two-dimensional, counter-flow diffusion flame established in the forward stagnation region of a porous cylinder, from the surface of which fuel gas is ejected uniformly into the uniform air stream. The effects of the aerodynamic and chemical parameters, such as the air stream velocity, the fuel ejection velocity, the cylinder diameter and the fuel composition, upon the location of the flame, the blow-off limit, the temperature distribution and the flow pattern of the flame, have been examined in detail. These experimental results and discussions are reported elsewhere, and it is suggested that this counter-flow diffusion flame can be used to study the flame strength and will also extend the range of applicability of flame-kinetics studies by structure analysis [*11*].

In order to evaluate the effects of the aerodynamic and chemical parameters upon the location of the counter-flow diffusion flame established in the forward stagnation region of a porous cylinder, a theoretical analysis has also been performed on a simplified model, and the concentration and temperature profiles across the flame and the flow pattern have been calculated. Such a calculation on a simplified model is presented in this paper. On completion of the analysis for the general system, numerical results are given for some representative reactions, and some of these theoretical results are compared with the observed results.

2. Brief Description of Experiment. Appearance of Observed Flame [*11*]

Before the model to be adopted in the present analysis is proposed, the appearance of the diffusion flame observed in the experiment is presented briefly. The experiment was performed using a rectangular combustion chamber of 3 cm×12 cm cross section and four kinds of uncooled porous cylinders of 3 cm long. The air was supplied from a blower through a settling chamber and a converging nozzle to the combustion chamber, and the air stream entering the combustion chamber presented a uniform velocity profile. The diameters of porous cylinders (sintered bronze) were 1.5, 3.0, 4.5 and 6.0 cm. The fuels used were propane and city gas. The location of the flame was measured by taking direct photographs and the flow pattern was recorded by photographing the tracks of small particles introduced into the air stream. The temperature distributions were measured with a Pt/Pt-Rh

thermocouple.

For appropriate conditions of the uniform air stream velocity V and the fuel ejection velocity v_w, a thin, laminar, two-dimensional blue flame was stabilized at some distance y_* from the cylinder surface in the forward stagnation region (Figure 1). As the fuel ejection velocity was decreased or the air stream velocity

(a) Direct photograph. (b) Instantaneous schlieren photograph.

FIG. 1. Counter-flow diffusion flame stabilized in the forward stagnation region of a porous cylinder. Propane-air flame. Cylinder diameter D, 3.0 cm. $V=150$ cm/sec. $v_w=3.1$ cm/sec.

was increased, the flame approached the cylinder surface, and finally the flame blew off from the stagnation region and was suddenly converted into the so-called wake flame. On the contrary, with the increase of v_w or with the decrease of V, y_* increased gradually. However, if v_w/V was greatly increased, large scale deformations appeared in the flame front and the laminar, two-dimensional flame was established no further.

In the special case when V was very small and v_w was comparatively large, the flame thickness increased remarkably and the flame showed luminous yellow inner (fuel side) and blue outer (air side) zones. In the limiting case of small V, the luminous yellow flame and the blue flame separated completely. In another extreme case when V was very large, the flame could not be stabilized in the forward stagnation region, however large the fuel ejection velocity was, and it was found that there exists a critical stagnation velocity gradient, $(2V/R)_c$, beyond which

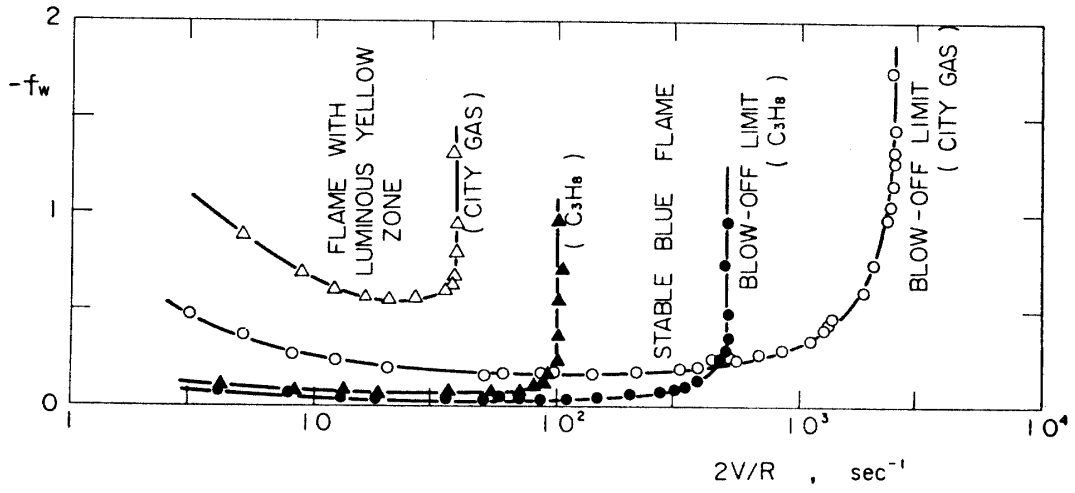

FIG. 2. Flame stability diagrams for propane-air and city gas-air flames. $D=3.0$ cm.

the flame can never be stabilized. This critical blow-off limit due to chemical limitations on the combustion rate was clearly discriminated from the blow-off due to thermal quenching of the flame.

An example of measured blow-off limits of propane-air flame and city gas-air flame is presented in Figure 2, in which the nondimensional ejection parameter $-f_w$ defined by $-f_w=(v_w/V)(R_e/2)^{\frac{1}{2}}$ is plotted against the stagnation velocity gradient $2V/R(R_e=VR/\nu$: the Reynolds number, ν: the mean kinematic viscosity across the boundary layer with flame in the stagnation region). In this figure, the limits at which the luminous yellow zone begins to appear in the flame are also plotted.

3. Formulation of the Combustion Problem

As the Reynolds number R_e is comparatively large and the flame is very thin except in the case when the luminous yellow zone appears in the flame, the flow and temperature fields may be analyzed approximately on the flame sheet model and by the boundary layer approximation. The flame sheet model of chemical reaction in the boundary layer has been considered by several authors [*12*]~[*17*]. In this model chemical reaction is confined to one or more discontinuity surfaces which are located within the boundary layer by requirements on the composition and/or temperature at the sheet, and the combustion process is completely controlled by the rate at which fuel and oxygen may diffuse to the flame front. Thus the flow is effectively frozen except at the sheet. Although the blow-off limit of the flame can not be predicted on the flame sheet model in which the infinite rate of reaction is assumed, this simple model has been used to predict the location of the flame in the boundary layer.

The model adopted in the present analysis is schematically shown in Figure 3. The fuel gas is ejected uniformly from the surface of a porous cylinder situated in the uniform air stream of velocity V, and a flame sheet is established within the boundary layer in the forward stagnation region of the cylinder. In this case the fuel gas is present in the region between the cylinder surface and the flame sheet, while oxygen is present only in the outer region of the boundary layer. The inert nitrogen and the combustion product will be present throughout the entire boundary layer.

For simplicity, the following assumptions are made for the analysis:

1. The flow is two-dimensional, steady and laminar.
2. Viscous dissipation and radiation are neglected.
3. The specific heat c_p at constant pressure is the same for all relevant chemical species and constant.
4. The chemical species in the boundary layer are the fuel gas (subscript 1), oxygen (subscript 2), nitrogen (subscript 3) and the combustion product (subscript 4).
5. The density ρ and the transport properties such as the viscosity μ, the thermal conductivity λ and the diffusion coefficient D of gas mixtures are constant.

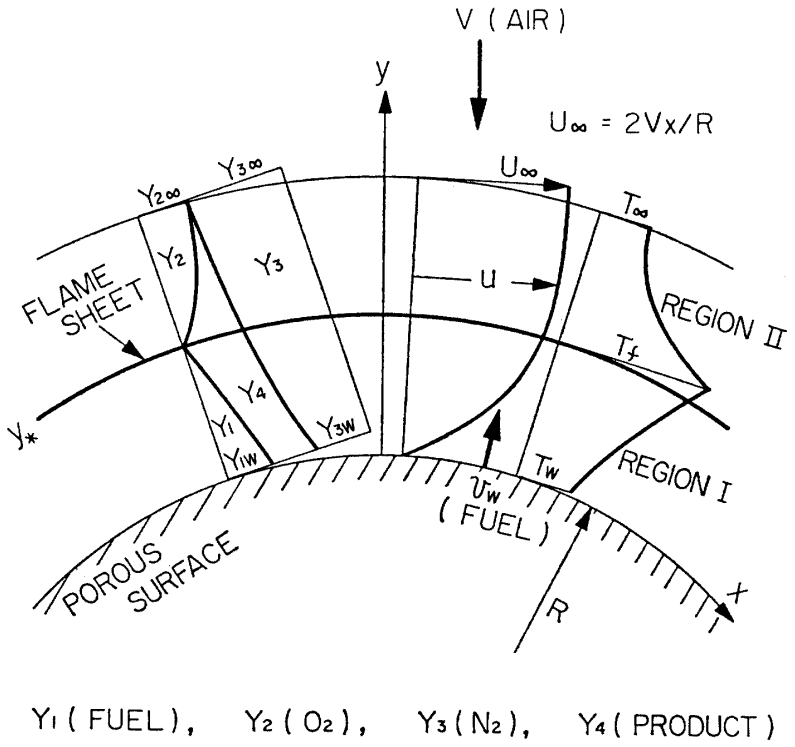

FIG. 3. Schematic diagram of counter-flow diffusion flame stabilized in the forward stagnation region of a porous cylinder.

6. Combustion process is completely diffusion controlled and results in a zero mass fraction for the fuel gas and oxygen at the flame sheet.

7. The correct proportions of the fuel gas and oxygen arrive at the flame sheet to provide a stoichiometric mixture.

A simple analysis of combustion in the boundary layer on the flame sheet model and under these assumptions was performed by Hartnett and Eckert in order to study the influence of combustion upon the mass transfer cooling of the skin of re-entering vehicles and the walls of rocket nozzles [*14*]. Their problem is substantially the same as the present problem of the counter-flow diffusion flame established in the forward stagnation region of a porous cylinder, except that the temperature of air at the outer edge of the boundary layer is very high. Therefore the analysis by Hartnett and Eckert may be adopted to the present problem without any substantial modification. In their analysis, however, the iterative method was used to determine the location of the flame, and therefore, the numerical calculation is somewhat troublesome. In the present paper, an improved method is presented, in which the general analytic expression for the relation between the location of the flame and the fuel ejection rate is obtained, and the location of the flame is determined for various combinations of reactants by a simple calculation.

4. GOVERNING EQUATIONS

Let the origin of the coordinate be at the stagnation point on the cylinder surface and the x- and y-axes be along and perpendicular to the surface, respectively.

The air of temperature T_∞, outside the boundary layer, flows at a velocity U_∞ $(=2Vx/R)$ parallel to the x axis (Figure 3). Denoting the velocity components in the x and y directions by u and v, respectively, the mass concentration (i.e., weight ratio) of i'th species by Y_i, and the local gas temperature by T, the resulting boundary layer equations may be written as follows:
Global continuity equation:

$$\frac{\partial u}{\partial x}+\frac{\partial v}{\partial y}=0. \tag{4.1}$$

Momentum equation:

$$u\frac{\partial u}{\partial x}+v\frac{\partial u}{\partial y}=U_\infty\frac{dU_\infty}{dx}+\nu\frac{\partial^2 u}{\partial y^2}. \tag{4.2}$$

Diffusion equation for each species:

$$u\frac{\partial Y_i}{\partial x}+v\frac{\partial Y_i}{\partial y}=D\frac{\partial^2 Y_i}{\partial y^2},\quad (i=1,\ 2,\ 3) \tag{4.3}\sim(4.5)$$

$$\sum_{i=1}^{4}Y_i=1. \tag{4.6}$$

Energy equation:

$$u\frac{\partial T}{\partial x}+v\frac{\partial T}{\partial y}=\kappa\frac{\partial^2 T}{\partial y^2}. \tag{4.7}$$

In these equations $\nu(=\mu/\rho)$ and $\kappa(=\lambda/c_p\rho)$ are the kinematic viscosity and the thermometric conductivity of gas mixtures, respectively. The term $u\dfrac{\partial p}{\partial x}$ has been neglected in the energy equation, because the kinetic energy is very small compared to the thermal enthalpy.

The boundary conditions of these governing equations are as follows:

$$\left.\begin{aligned}&\text{at } y=0: u=0,\ v=v_w,\ Y_1=Y_{1w},\ Y_3=Y_{3w},\ T=T_w,\\&\text{as } y\to\infty: u\to U_\infty,\ Y_2\to Y_{2\infty},\ Y_3\to Y_{3\infty},\ T\to T_\infty,\\&\text{at } y=y_* \text{ (at flame sheet)}: Y_1=0,\ Y_2=0,\ T=T_f.\end{aligned}\right\} \tag{4.8}$$

The above equations and the boundary conditions are sufficient to determine the velocity, concentration and temperature profiles, if v_w, Y_{iw}, T_f and y_* are specified. As is well known, however, in the boundary layer problem with foreign gas injection, Y_{iw} cannot be specified independently of v_w[*18*] [*19*], and the flame temperature and the location of the flame are also functions of v_w and the fuel composition [*14*]. Y_{iw}, y_* and T_f are determined respectively by the following conditions.

In general, the velocity v_i in the y direction of the i'th species is composed of a diffusion velocity $-(D/Y_i)(\partial Y_i/\partial y)$ and a convection velocity v, i.e.,

$$Y_i v_i = -D\left(\frac{\partial Y_i}{\partial y}\right) + Y_i v\,. \tag{4.9}$$

It is reasonable to put the physical condition that there is to be no net flow of the gas components except the ejected fuel gas through the cylinder surface. Therefore, v_{3w} and v_{4w} are 0 and the relations

$$D(\partial Y_3/\partial y)_w = Y_{3w} v_w \tag{4.10}$$

and

$$D(\partial Y_4/\partial y)_w = Y_{4w} v_w \tag{4.11}$$

exist for the inert nitrogen and the combustion product. Substituting for Y_4 the expression obtained from Equation (4.6) and noting that no oxidizer appears at the surface, Equations (4.10) and (4.11) may be combined to yield

$$-D(\partial Y_1/\partial y)_w = (1 - Y_{1w}) v_w\,. \tag{4.12}$$

The resulting convection velocity v_w at the surface of the cylinder is the velocity associated with the momentum equation and, therefore, Equations (4.10)~(4.12) give the relationship between the ejection velocity and the concentration of each species at the cylinder surface, i.e., Y_{iw} is determined when the ejection velocity is specified.

Since at the flame sheet fuel and oxygen are in stoichiometric ratio and since the diffusion coefficients are assumed to be the same for all relevant chemical species, it follows that at the flame sheet

$$\left(\frac{\partial c_1}{\partial y}\right)_{y*} = -\frac{1}{i}\left(\frac{\partial c_2}{\partial y}\right)_{y*}, \tag{4.13}$$

where c_1 and c_2 are the mole concentrations (number of moles in unit volume) of fuel and oxygen, respectively, and i is the number of moles of oxygen required to burn 1 mole of fuel to effect complete combustion. If j is the number of grams of oxygen required to burn 1 gram of fuel to effect complete combustion, the condition (4.13) can be rewritten as

$$\left(\frac{\partial Y_1}{\partial y}\right)_{y*} = -\frac{1}{j}\left(\frac{\partial Y_2}{\partial y}\right)_{y*}, \tag{4.14}$$

in which $j = i m_2/m_1$ and m_1 and m_2 are the molecular weights of fuel and oxygen, respectively. Equation (4.14) gives the relationship between the ejection velocity and the location of the flame.

The temperature T_f at the flame sheet is determined by the requirement that the energy generated by the combustion process must be equal to the heat flow away from the flame sheet by conduction, i.e.,

$$\lambda\left(\frac{\partial T_I}{\partial y}\right)_{y*} - \lambda\left(\frac{\partial T_{II}}{\partial y}\right)_{y*} = -D\left(\frac{\partial Y_1}{\partial y}\right)_{y*} H, \tag{4.15}$$

in which T_I and T_{II} are the local gas temperatures for the region between the cylinder surface and the flame sheet (say, region I) and for the region outside the flame sheet (say, region II), respectively, and H is the heat of combustion per unit volume of fuel. The first term in Equation (4.15) represents the heat flow away from the flame sheet toward the cylinder surface, while the second term is the heat conducted toward the outer edge of the boundary layer.

Introducing these additional conditions (4.10), (4.11), (4.12), (4.14) and (4.15), the specification of the ejection velocity v_w and the composition of fuel uniquely determines the problem.

5. Analysis

5-1. Solution of Momentum Equation

As is well known, the global continuity equation and the momentum equation may be transformed to an ordinary differential equation by introducing the stream function ψ, defined by the usual relations

$$u=\frac{\partial \psi}{\partial y}, \quad v=-\frac{\partial \psi}{\partial x}, \tag{5.1}$$

as well as the following dimensionless variables

$$\psi(x, \eta)=\sqrt{U_\infty \nu x}\, f(\eta), \quad \eta=\sqrt{U_\infty/\nu x}\, y. \tag{5.2}$$

Equations (4.1) and (4.2) then become

$$f'''+ff''-(f')^2+1=0, \tag{5.3}$$

in which primes denote differentiation with respect to η. The appropriate boundary conditions are as follows:

$$\left.\begin{aligned} &\text{at } \eta=0 : f'=0,\ f=f_w=-\frac{v_w}{V}\sqrt{\frac{R_e}{2}}, \\ &\text{as } \eta\to\infty : f'\to 1, \end{aligned}\right\} \tag{5.4}$$

in which $R_e=VR/\nu$. The solution of Equation (5.3), subject to the imposed boundary conditions, has been reported in several references and recently in more detail by Hayasi for a range of ejection rates, f_w [20].

5-2. Solution of Diffusion Equation for Each Species. Location of Flame Sheet

In order to determine the concentration profile of each species, it is necessary to solve three diffusion equations (4.3), (4.4) and (4.5) with the boundary con-

ditions (4.8) and the subsidiary conditions (4.10), (4.12) and (4.14). But the location of the flame is not determined previously, so that one of the boundary conditions is indeterminate. Hartnett and Eckert used the iterative method to determine the location of the flame sheet, and therefore, the numerical calculation is rather troublesome. This difficulty, however, can be easily overcome by the following simple device which was first proposed by Burke and Schumann and has been used by many authors for the studies of diffusion flames [*21*].

As j is grams of oxygen required to burn 1 gram of fuel to effect complete combustion, Y_2/j represents the equivalent fuel concentration. Since at the flame sheet fuel and oxygen are in stoichiometric ratio and since the diffusion coefficients are assumed to be the same for all relevant chemical species, it follows that

$$\left(\frac{\partial Y_1}{\partial y}\right)_{y_*} = \left\{\frac{\partial}{\partial y}\left(\frac{-Y_2}{j}\right)\right\}_{y_*}. \tag{4.14}$$

Thus, in Figure 4 the reflected or mirror image curve $-Y_2/j$ connects smoothly with the fuel concentration curve at the flame sheet; and since the fuel concentration curve and the reflected curve are both determined by the same diffusion equation,

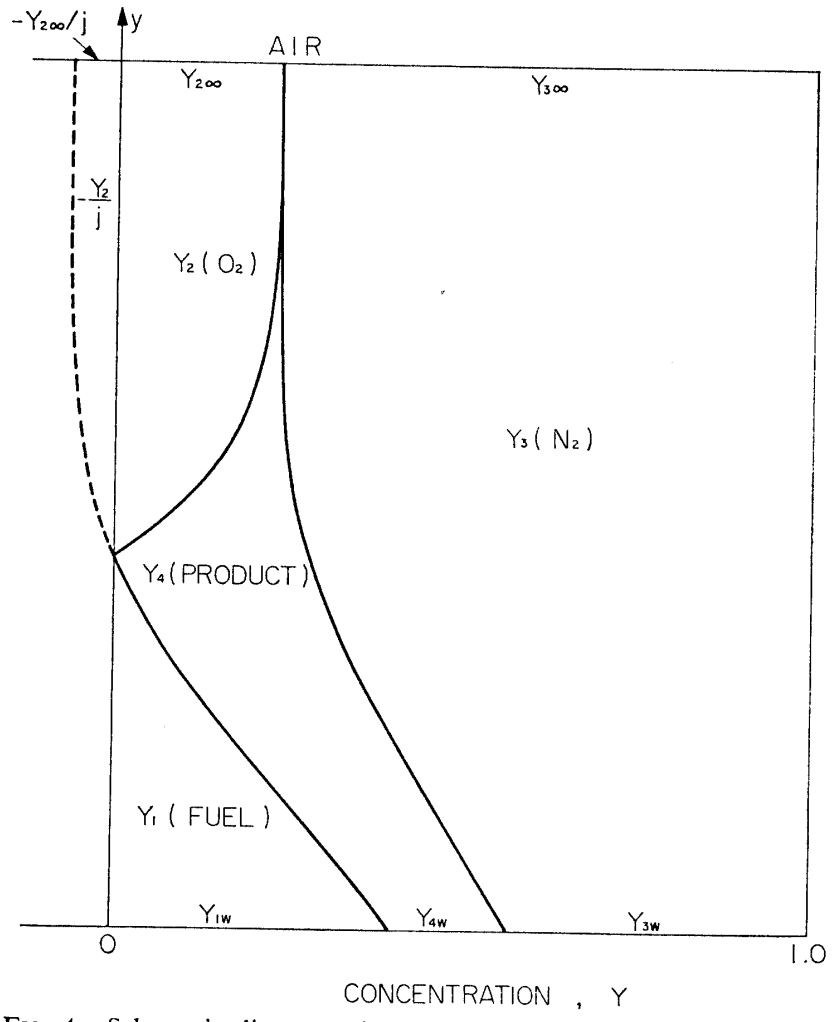

FIG. 4. Schematic diagram of concentration profiles across the flame.

the reflected curve may be considered, for mathematical purposes, to represent negative concentrations of fuel having a maximum value (largest negative value) at the outer edge of the boundary layer and a value of zero at the flame sheet. The diffusion problem of fuel and oxygen then reduces to the diffusion of a single gas, namely fuel gas. Therefore the diffusion equations to be solved to determine the concentration profile of each species are

$$u\frac{\partial Y_1}{\partial x}+v\frac{\partial Y_1}{\partial y}=D\frac{\partial^2 Y_1}{\partial y^2}, \tag{4.3}$$

and

$$u\frac{\partial Y_3}{\partial x}+v\frac{\partial Y_3}{\partial y}=D\frac{\partial^2 Y_3}{\partial y^2}. \tag{4.5}$$

The boundary conditions of these equations are

$$\left.\begin{aligned}&\text{at } y=0 : Y_1=Y_{1w},\ Y_3=Y_{3w},\\&\text{as } y\to\infty : Y_1\to -Y_{2\infty}/j,\ Y_3\to Y_{3\infty}.\end{aligned}\right\} \tag{5.5}$$

The location of the flame sheet y_* can be immediately determined by the condition that Y_1 is zero.

If we put

$$\phi_1(\eta)=\frac{Y_1+\dfrac{Y_{2\infty}}{j}}{Y_{1w}+\dfrac{Y_{2\infty}}{j}}, \tag{5.6}$$

and

$$\phi_3(\eta)=\frac{Y_3-Y_{3w}}{Y_{3\infty}-Y_{3w}}, \tag{5.7}$$

Equations (4.3) and (4.5) are transformed to the ordinary differential equations,

$$\phi_1''+Sf\phi_1'=0, \tag{5.8}$$

and

$$\phi_3''+Sf\phi_3'=0, \tag{5.9}$$

respectively, in which $S(=\nu/D)$ is the Schmidt number. The boundary conditions are

$$\left.\begin{aligned}&\text{at } \eta=0 : \phi_1=1,\ \phi_3=0,\\&\text{as } \eta\to\infty : \phi_1\to 0,\ \phi_3\to 1.\end{aligned}\right\} \tag{5.10}$$

The solutions of these eqution which satisfy the boundary conditions are

$$\phi_1=1-\frac{\int_0^{\eta}\exp\left(-\int_0^{\eta}Sfd\eta\right)d\eta}{\int_0^{\infty}\exp\left(-\int_0^{\eta}Sfd\eta\right)d\eta}, \tag{5.11}$$

and

$$\phi_3=\frac{\int_0^{\eta}\exp(-\int_0^{\eta}Sfd\eta)d\eta}{\int_0^{\infty}\exp(-\int_0^{\eta}Sfd\eta)d\eta}, \tag{5.12}$$

respectively. The numerical integration of ϕ_3 has recently been carried out by Hayasi and values of ϕ_3 are presented in detail for a range of f_w and for S of 0.9 and 1.0 [*20*]. Substituting Equation (5.12) into Equation (4.10), the concentration of nitrogen at the cylinder surface, and accordingly the concentration profile of nitrogen within the boundary layer can be determined, i.e.,

$$Y_{3w}=\frac{Y_{3\infty}}{1-Sf_w\Lambda_s(\infty, f_w)}, \tag{5.13}$$

and

$$Y_3=Y_{3\infty}\left[\frac{1-Sf_w\Lambda_s(\eta, f_w)}{1-Sf_w\Lambda_s(\infty, f_w)}\right], \tag{5.14}$$

in which

$$\Lambda_s(\eta, f_w)=\int_0^{\eta}\exp(-\int_0^{\eta}Sfd\eta)d\eta, \tag{5.15}$$

and

$$\Lambda_s(\infty, f_w)=\int_0^{\infty}\exp(-\int_0^{\eta}Sfd\eta)d\eta. \tag{5.16}$$

It is easily found that the concentration profile of nitrogen depends on the Schmidt number S and the nondimensional ejection parameter f_w only and is independent of the composition of fuel.

Substituting Equation (5.11) into Equation (4.12), the concentration of fuel at the cylinder surface can be determined, i.e.,

$$Y_{1w}=\frac{-Sf_w\Lambda_s(\infty, f_w)-\dfrac{Y_{2\infty}}{j}}{1-Sf_w\Lambda_s(\infty, f_w)}. \tag{5.17}$$

The value of f_w is negative in the case of gas ejection from the surface. Therefore Y_{1w} becomes zero at a small, finite value of $-f_w$. This condition corresponds to stoichiometric combustion immediately on the surface. If the ejection velocity of fuel is smaller than this critical value, the combustion occurs directly on the surface but in the presence of excess oxygen. Such surface combustion was considered by several authors. As the ejection velocity of fuel is increased, and if

$$-Sf_w\Lambda_s(\infty, f_w)>\frac{Y_{2\infty}}{j}, \tag{5.18}$$

Y_{1w} becomes positive, and the flame front lifts off the surface and the flame sheet is established within the boundary layer. As shown in Figure 2, however, the surface combustion does not occur actually in the experiment, because the flame blows off from the stagnation region due to thermal quenching as the flame approaches the cylinder surface.

Substituting Equations (5.11) and (5.17) into Equation (5.6), the concentration profile of fuel within the boundary layer can be obtained, i.e.,

$$Y_1=\frac{-Sf_w\{\Lambda_s(\infty, f_w)-\Lambda_s(\eta, f_w)\}-\frac{Y_{2\infty}}{j}\{1-Sf_w\Lambda_s(\eta, f_w)\}}{1-Sf_w\Lambda_s(\infty, f_w)}. \tag{5.19}$$

If we put $Y_1=0$, the location of the flame sheet, η_*, can be determined immediately from the relation,

$$-Sf_w\{\Lambda_s(\infty, f_w)-\Lambda_s(\eta_*, f_w)\}-\frac{Y_{2\infty}}{j}\{1-Sf_w\Lambda_s(\eta_*, f_w)\}=0, \tag{5.20}$$

i.e.,

$$\Lambda_s(\eta_*, f_w)=\frac{\Lambda_s(\infty, f_w)+\frac{Y_{2\infty}/j}{Sf_w}}{1+\frac{Y_{2\infty}}{j}}. \tag{5.21}$$

It is easily found that the location of the flame sheet depends on the reaction parameter j as well as the Schmidt number S and the nondimensional ejection parameter f_w. Substituting Equation (5.21) into Equation (5.14), the concentration of nitrogen at the flame sheet can be obtained, i.e.,

$$Y_3(\eta_*)=\frac{Y_{3\infty}}{1+\frac{Y_{2\infty}}{j}}. \tag{5.22}$$

It must be noticed that at the flame sheet the concentration of nitrogen and accordingly the concentration of the combustion product depend on the reaction parameter j only and are independent of f_w.

5-3. Solution of Energy Equation

The solution to the energy equation (4.7) is required if the temperature distributions within the boundary layer are to be determined and the heat transfer to the surface is to be examined.

If we put

$$\theta_I(\eta)=\frac{T_I-T_w}{T_f-T_w} \tag{5.23}$$

for region I, and

$$\theta_{II}(\eta)=\frac{T_{II}-T_f}{T_\infty-T_f} \tag{5.24}$$

for region II, and if we assume that θ_I and θ_{II} are functions of η only, Equation (4.7) can be transformed to the ordinary differential equations,

$$\theta_I''+\sigma f\theta_I'=0 \tag{5.25}$$

for region I, and

$$\theta_{II}''+\sigma f\theta_{II}'=0 \tag{5.26}$$

for region II, in which $\sigma(=\nu/\kappa)$ is the Prandtl number. The boundary conditions are

$$\left.\begin{aligned} &\text{at } \eta=0 : \theta_I=0, \\ &\text{at } \eta=\eta_*: \theta_I=1,\ \theta_{II}=0, \\ &\text{as } \eta\to\infty: \theta_{II}\to 1. \end{aligned}\right\} \tag{5.27}$$

The solutions of these equations which satisfy the boundary conditions are

$$\theta_I=\frac{\Lambda_\sigma(\eta, f_w)}{\Lambda_\sigma(\eta_*, f_w)}, \tag{5.28}$$

and

$$\theta_{II}=\frac{\Lambda_\sigma(\eta, f_w)-\Lambda_\sigma(\eta_*, f_w)}{\Lambda_\sigma(\infty, f_w)-\Lambda_\sigma(\eta_*, f_w)}, \tag{5.29}$$

respectively, in which

$$\Lambda_\sigma(\eta, f_w)=\int_0^\eta \exp\left(-\int_0^\eta \sigma f d\eta\right)d\eta, \tag{5.30}$$

$$\Lambda_\sigma(\eta_*, f_w)=\int_0^{\eta_*} \exp\left(-\int_0^\eta \sigma f d\eta\right)d\eta, \tag{5.31}$$

and

$$\Lambda_\sigma(\infty, f_w)=\int_0^\infty \exp\left(-\int_0^\eta \sigma f d\eta\right)d\eta. \tag{5.32}$$

If we put

$$\Gamma_\sigma(\eta, f_w)=\frac{\Lambda_\sigma(\eta, f_w)}{\Lambda_\sigma(\infty, f_w)}, \tag{5.33}$$

and

$$\Gamma_\sigma(\eta_*, f_w)=\frac{\Lambda_\sigma(\eta_*, f_w)}{\Lambda_\sigma(\infty, f_w)}, \tag{5.34}$$

θ_I and θ_{II} can be expressed as

$$\theta_I=\frac{\Gamma_\sigma(\eta, f_w)}{\Gamma_\sigma(\eta_*, f_w)}, \tag{5.35}$$

and

$$\theta_{II}=\frac{\Gamma_\sigma(\eta, f_w)-\Gamma_\sigma(\eta_*, f_w)}{1-\Gamma_\sigma(\eta_*, f_w)}, \tag{5.36}$$

respectively.

Substituting Equations (5.11), (5.35) and (5.36) into Equation (4.15), the temperature T_f at the flame sheet can be determined, i.e.,

$$T_f=T_w+(T_\infty-T_w)\Gamma_\sigma(\eta_*, f_w)+\frac{H}{\rho c_p}\left(Y_{1w}+\frac{Y_{2\infty}}{j}\right)\Gamma_\sigma(\eta_*, f_w)$$
$$\times\{1-\Gamma_\sigma(\eta_*, f_w)\}L_e\frac{\Gamma_s'(\eta_*, f_w)}{\Gamma_\sigma'(\eta_*, f_w)}. \tag{5.37}$$

In the case when the Lewis number $L_e(=\sigma/S)$ is 1,

$$L_e \frac{\Gamma_s'(\eta_*, f_w)}{\Gamma_\sigma'(\eta_*, f_w)} = 1 . \tag{5.38}$$

Therefore the flame temperature becomes

$$T_f = T_w + (T_\infty - T_w)\Gamma_1(\eta_*, f_w) + \frac{H}{\rho c_p}\left(Y_{1w} + \frac{Y_{2\infty}}{j}\right)\Gamma_1(\eta_*, f_w) \times \{1 - \Gamma_1(\eta_*, f_w)\} , \tag{5.39}$$

in which

$$\Gamma_1(\eta_*, f_w) = \frac{\Lambda_1(\eta_*, f_w)}{\Lambda_1(\infty, f_w)} = \frac{\int_0^{\eta_*} \exp\left(-\int_0^\eta f d\eta\right) d\eta}{\int_0^{\infty} \exp\left(-\int_0^\eta f d\eta\right) d\eta} . \tag{5.40}$$

The heat flow to the cylinder surface with combustion occurring in the stagnation region may be determined from the relation,

$$q = \lambda\left(\frac{\partial T_1}{\partial y}\right)_w , \tag{5.41}$$

in which q is the heat flow per unit area and time. Substituting Equation (5.35) into Equation (5.41), we obtain

$$\frac{q \cdot R}{\lambda\sqrt{2R_e}\,(T_f - T_w)} = \left(\frac{d\theta_1}{d\eta}\right)_w = \frac{\Gamma_\sigma'(0, f_w)}{\Gamma_\sigma(\eta_*, f_w)} = \frac{1}{\Lambda_\sigma(\eta_*, f_w)} . \tag{5.42}$$

In the preceding section, the location of the flame sheet was determined as a function of f_w. It then follows from the above equations that the specification of T_w and T_∞ completely determines the temperature distribution throughout the boundary layer and the heat flow to the cylinder surface.

6. Numerical Examples

The present analysis has been applied to the combustion situations shown in Table 1 and numerical calculations have been carried out by manual computation for $S = \sigma = 1$. In this calculation, the numerical solutions of $f(\eta)$ and $\Lambda_1(\eta, f_w)$ obtained by Hayasi have been used, and the concentrations of oxygen and nitrogen in air, i.e., $Y_{2\infty}$ and $Y_{3\infty}$, have been assumed to be 0.233 and 0.767, respectively.

The resulting location of the flame sheet, designated as η_*, is shown in Figures 5 and 6. In Figure 5, η_* is presented as functions of $-f_w$, j being the parameter, while in Figure 6, η_* is presented as functions of j, $-f_w$ being the parameter. The location of the stagnation point η_s is also presented in Figure 5. It is seen that the value of η_* starts with a zero value at a finite fuel ejection velocity for each of the reactions considered. As already pointed out, this condition corresponds to the stoichiometric combustion immediately on the surface. A small increase in the ejection rate of fuel above the value required for stoichiometric surface combustion causes an appreciable movement of the flame sheet into the boundary layer. η_* increases with increasing $-f_w$ and j, and the flame sheet lies always on the air

TABLE 1.

Fuel	Chemical reaction	i	m_1	m_2	m_2/m_1	j
H_2	$H_2+\frac{1}{2}O_2\rightarrow H_2O$	0.5	2	32	16	8
C	$C+O_2\rightarrow CO_2$	1	12	32	8/3	2.667
C	$C+\frac{1}{2}O_2\rightarrow CO$	0.5	12	32	8/3	1.333
CO	$CO+\frac{1}{2}O_2\rightarrow CO_2$	0.5	28	32	8/7	0.5714
CH_4	$CH_4+2O_2\rightarrow CO_2+2H_2O$	2	16	32	2	4
C_2H_6	$C_2H_6+3\frac{1}{2}O_2\rightarrow 2CO_2+3H_2O$	3.5	30	32	16/15	3.733
C_3H_8	$C_3H_8+5O_2\rightarrow 3CO_2+4H_2O$	5	44	32	8/11	3.636
C_2H_2	$C_2H_2+2\frac{1}{2}O_2\rightarrow 2CO_2+H_2O$	2.5	26	32	16/13	3.077
C_2H_4	$C_2H_4+3O_2\rightarrow 2CO_2+2H_2O$	3	28	32	8/7	3.429
City gas	City gas$+0.908\,O_2\rightarrow\alpha CO_2+\beta H_2O$	0.908	17.05	32	1.877	1.704

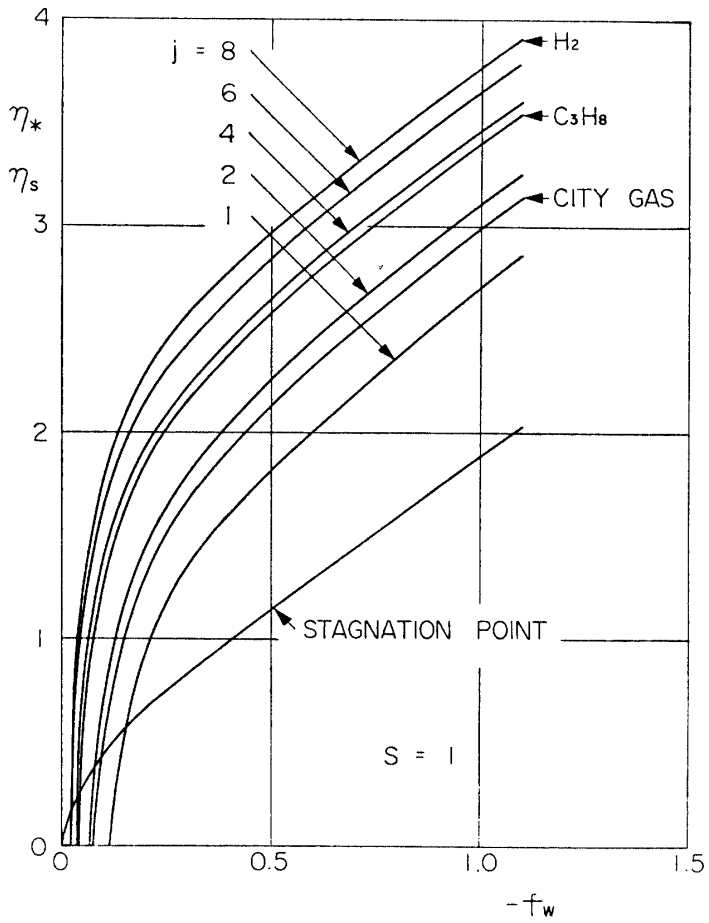

FIG. 5. Location of flame sheet η_* and location of stagnation point η_s as functions of fuel ejection rate $-f_w$.

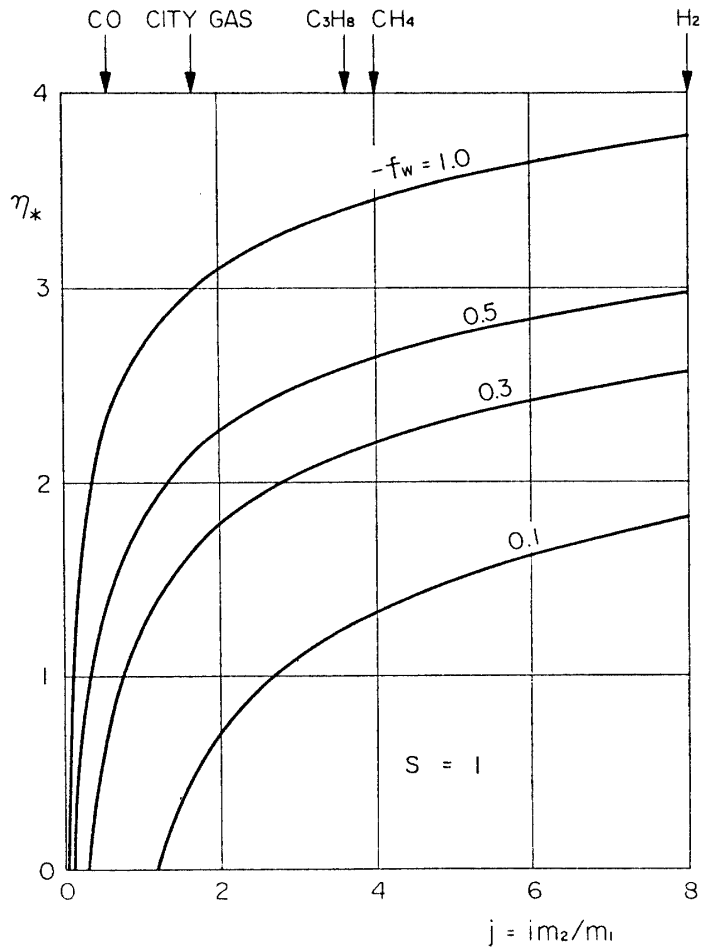

FIG. 6. Location of flame sheet η_* as functions of reaction parameter j.

side of the stagnation point except in the case of extremely small $-f_w$. It has been confirmed that the numerical results of the present analysis are completely consistent with those obtained through the iterative method by Hartnett and Eckert [*14*].

The concentration profiles and the temperature distributions across the boundary layer are presented in Figures 7 and 8, respectively, for propane combustion with the ejection rates, $-f_w$, equal to 0.1, 0.5 and 1.0. It may be seen in these figures that the flame sheet is located relatively far from the surface and close to the outer edge of the boundary layer if the ejection rate is comparatively large. The non-dimensional heat flows to the cylinder surface with and without combustion in the stagnation region are presented in Figure 9.

7. Comparison with Experimental Results

The measured locations of thin, blue flames of propane-air and city gas-air are shown in Figure 10, in which the nondimensional distance η_* is plotted against the nondimensional ejection parameter $-f_w$ [*11*]. It is found that the measured distance η_* is completely correlated with $-f_w$ independent of V and v_w for a given

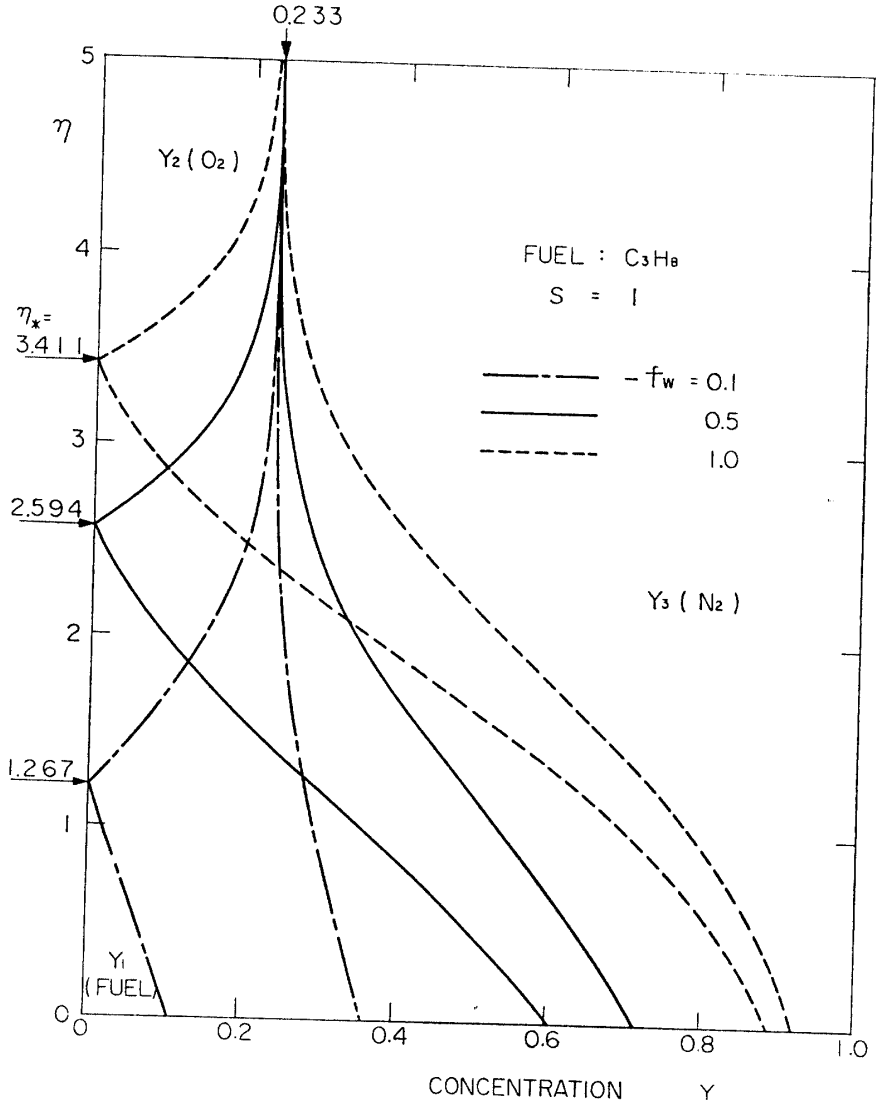

FIG. 7. Concentration profiles across the propane-air flame. $-f_w$=0.1, 0.5 and 1.0. S=1.

combination of reactants and the cylinder of a fixed diameter, and the distance η_* for propane-air flame is larger than that for city gas-air flame. The calculated locations of propane-air flame, city gas-air flame and the stagnation point are also presented in this figure. The theoretical results obtained in the present analysis are found to be qualitatively consistent with the observed results.

Figure 11 shows an example of particle streak picture of the stagnation flow with flame. The particles introduced into the air stream always passed through the flame and the stagnation point was found to be on the fuel side of the flame. The theoretical prediction that the flame should lie on the air side of the stagnation point except in the case of extremely small $-f_w$ was strikingly confirmed for both propane-air and city gas-air flames.

These experimental results suggest that the flame sheet model is useful to evaluate the effects of the aerodynamic and chemical parameters upon the location of

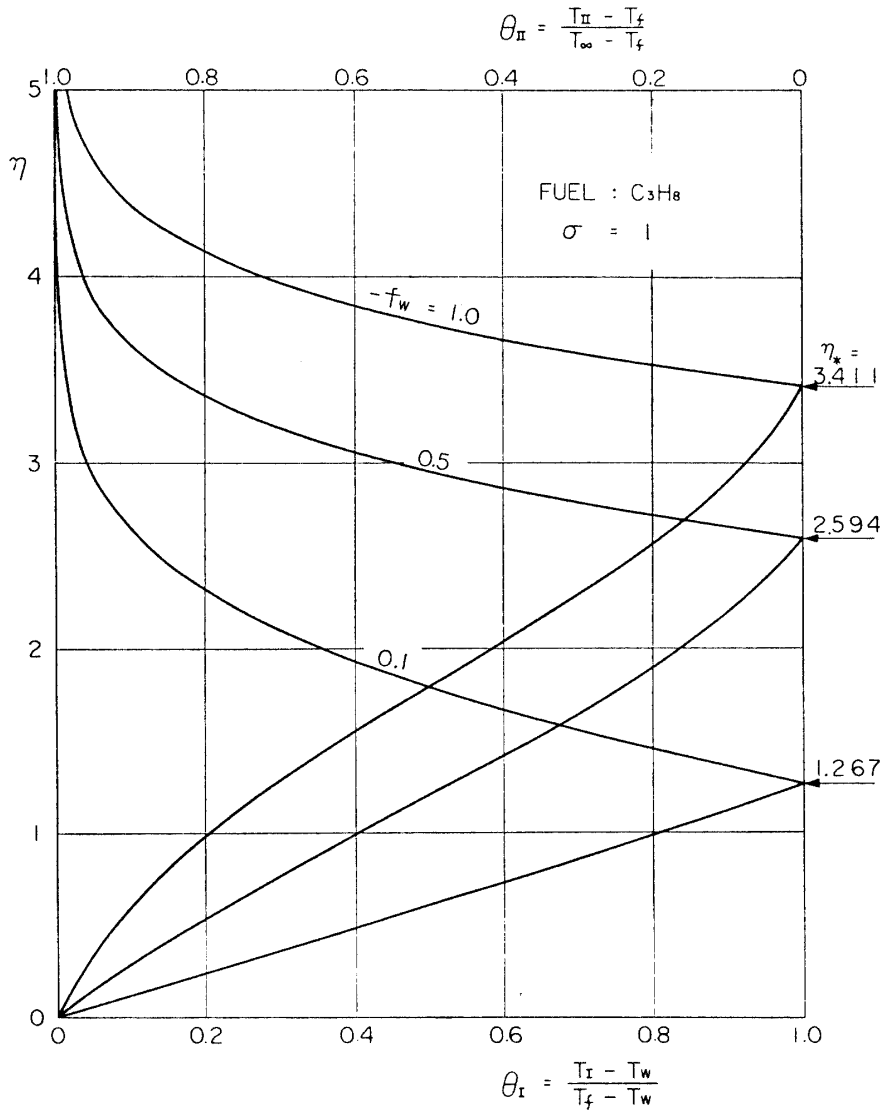

FIG. 8. Temperature profiles across the propane-air flame. $-f_w$=0.1, 0.5 and 1.0. σ=1.

the flame and the flow field, etc., although the blow-off limit of the flame observed in the experiment can not be predicted on the flame sheet model in which the infinite rate of reaction is assumed in the flame.

8. Concluding Remarks

In the present paper, the counter-flow diffusion flame established in the forward stagnation region of a porous cylinder has been analyzed on the simple flame sheet model and by the boundary layer approximation, and the effects of the aerodynamic and chemical parameters upon the location of the flame have been examined. The general analytic expressions of the location of the flame and the concentration and temperature profiles across the flame have been obtained as functions of the fuel ejection rate and the fuel composition, and the location of the flame has been

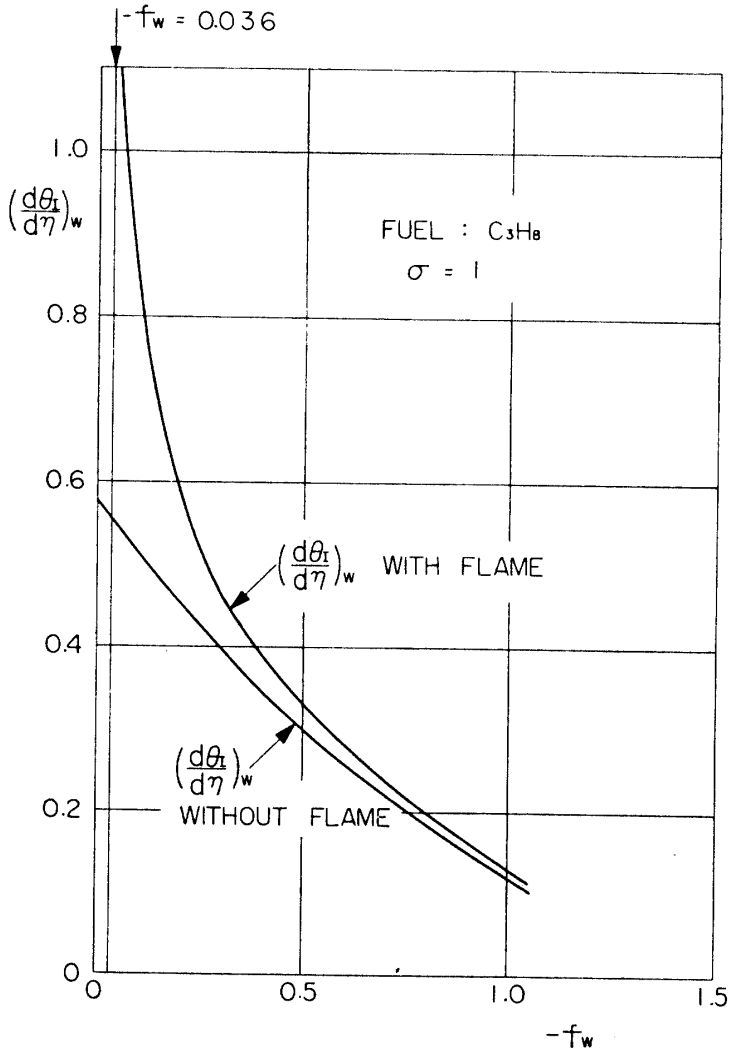

FIG. 9. Heat flow to the cylinder surface with and without combustion. Propane-air flame.

calculated for various combinations of reactants. It has been confirmed that the theoretical results are qualitatively consistent with the experimental results and the flame sheet model is useful to predict the location of the counter-flow diffusion flame established in the forward stagnation region of a porous cylinder.

The authors would like to express their sincere thanks to Dr. N. Hayasi for his kind advice in numerical calculation.

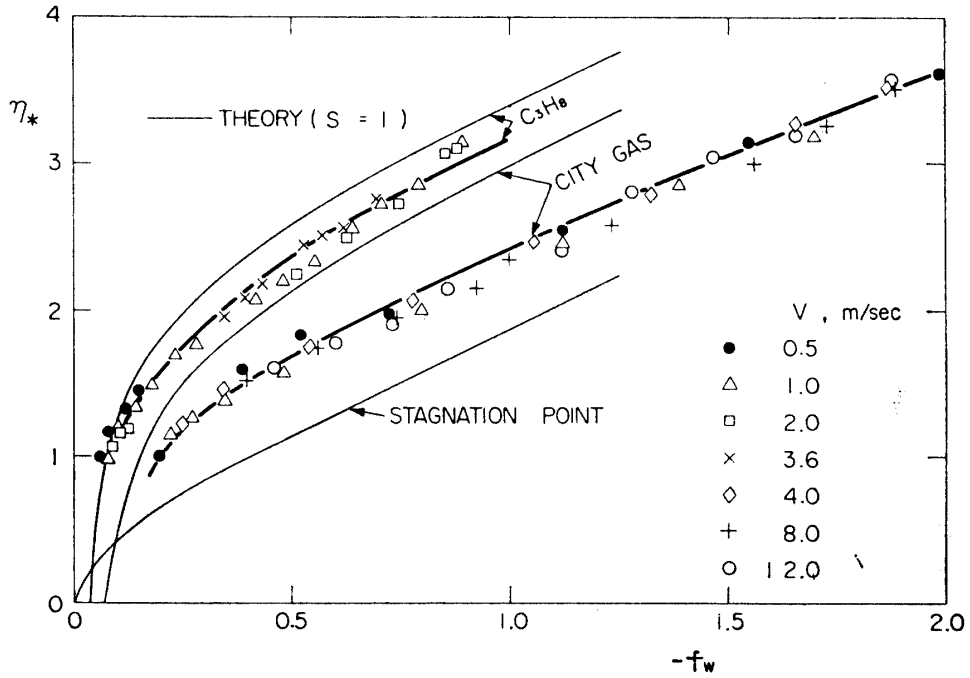

FIG. 10. Measured locations of propane-air and city gas-air flames. $D=3.0$ cm.

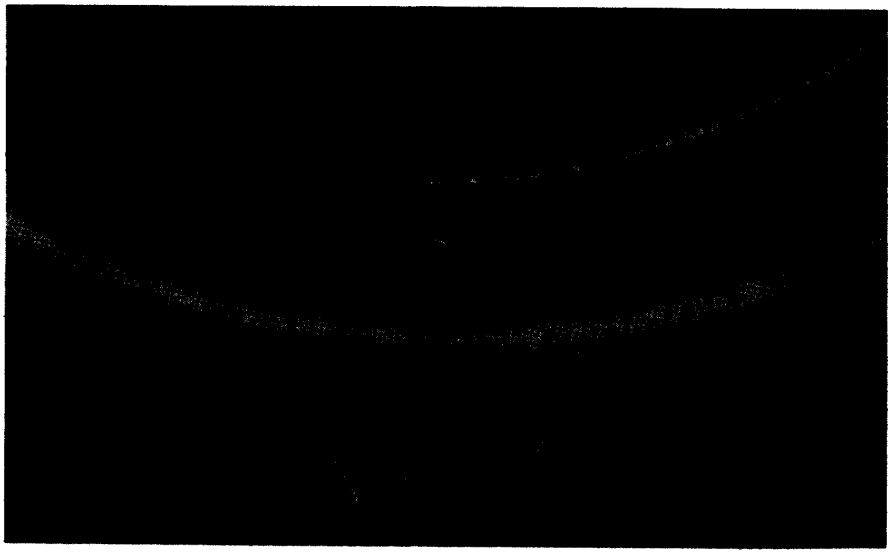

FIG. 11. Particle streak picture of counter-flow diffusion flame. Propane-air flame. $D=3.0$ cm. $V=80$ cm/sec. $v_w=8.6$ cm/sec.

Department of Jet Propulsion,
Institute of Space and Aeronautical Science,
University of Tokyo, Tokyo
June 8, 1966

References

[*1*] D. B. Spalding: Experiments on the burning and extinction of liquid fuel spheres, Fuel, Vol. 32, No. 2 (1953), pp. 169/185.

[*2*] D. B. Spalding: The combustion of liquid fuels, Fourth Intern. Symp. on Combustion, Williams and Wilkins, Baltimore (1953), pp. 847/864.

[*3*] D. B. Spalding: A theory of the extinction of diffusion flames, Fuel, Vol. 33, No. 3 (1954), pp. 255/273.

[*4*] F. E. Fendell: Ignition and extinction in combustion of initially unmixed reactants, Journ. Fluid Mech., Vol. 21, Pt. 2 (1965), pp. 281/303.

[*5*] A. E. Potter, Jr. and J. N. Butler: A novel combustion measurement based on the extinguishment of diffusion flames, ARS Journ., Vol. 29, No. 1 (1959), pp. 54/56.

[*6*] A. E. Potter, Jr., S. Heimel and J. N. Butler: Apparent flame strength. A measure of maximum reaction rate in diffusion flames, Eighth Intern. Symp. on Combustion, Williams and Wilkins, Baltimore (1962), pp. 1027/1034.

[*7*] E. Anagnostou and A. E. Potter: Flame strength of propane-oxygen flames at low pressures in turbulent flow, Ninth Intern. Symp. on Combustion, Academic Press, New York (1963), pp. 1/6.

[*8*] D. B. Spalding: Theory of mixing and chemical reaction in the opposed-jet diffusion flame, ARS Journ., Vol. 31, No. 6 (1961), pp. 763/771.

[*9*] T. P. Pandya and F. J. Weinberg: The study of the structure of laminar diffusion flames by optical methods, Ninth Intern. Symp. on Combustion, Academic Press, New York (1963), pp. 587/596.

[*10*] T. P. Pandya and F. J. Weinberg: The structure of flat, counter-flow diffusion flames, Proc. Roy. Soc., London, A, Vol. 279, No. 1379 (1964), pp. 544/561.

[*11*] H. Tsuji and I. Yamaoka: The counter-flow diffusion flame in the forward stagnation region of a porous cylinder, to be presented at the Eleventh Intern. Symp on Combustion, University of California, Berkeley (1966).

[*12*] G. W. Sutton: Combustion of a gas injected into a hypersonic boundary layer, Seventh Intern. Symp. on Combustion, Butterworths, London (1959), pp. 539/545.

[*13*] L. Lees: Convective heat transfer with mass addition and chemical reactions, Combustion and Propulsion, Third AGARD Colloq., Pergamon, New York (1958), pp. 451/498.

[*14*] J. P. Hartnett and E. R. G. Eckert: Mass transfer cooling with combustion in a laminar boundary layer, 1958 Heat Transfer and Fluid Mech. Inst., Stanford Univ. Press, Stanford (1958), pp. 54/68.

[*15*] C. B. Cohen, R. Bromberg and R. P. Lipkis: Boundary layers with chemical reactions due to mass addition, Jet Propulsion, Vol. 28, No. 10 (1958), pp. 659/668.

[*16*] R. Bromberg and R. P. Lipkis: Heat transfer in boundary layers with chemical reactions due to mass addition, Jet Propulsion, Vol. 28, No. 10 (1958), pp. 668/674.

[*17*] A. Q. Eschenroeder: Combustion in the boundary layer on a porous surface, Journ. Aero. Sci., Vol. 27, No. 12 (1960), pp. 901/906.

[*18*] H. Tsuji: Ignition and flame stabilization in the laminar boundary layer on a porous flat plate with hot gas injection, Aero. Res. Inst., Univ. of Tokyo, Report No. 365 (1961).

[*19*] H. Tsuji: An aerothermochemical analysis of erosive burning of solid propellant, Ninth Intern. Symp. on Combustion, Academic Press, New York (1963), pp. 384/393.

[*20*] N. Hayasi: On stagnation flows with blowing, to be presented at Fifth U.S. Nat. Congr. Appl. Mech., June 14–17 (1966).

[*21*] S. P. Burke and T. E. W. Schuman: Diffusion flames, Ind. Eng. Chem., Vol. 20, No. 10 (1928), pp. 998/1004; or Proc. First and Second Symp. on Combustion, The Combustion Inst., Pittsburgh (1965), pp. 2/11.